^{11}C-raclopride and that of ^{11}C-CFT in the three subregions of the striatum. The URI of ^{11}C-CFT was smaller in the following order: the posterior putamen < anterior putamen < caudate, whereas the URI of ^{11}C-raclopride was larger as follows: the posterior putamen > anterior putamen > caudate. In contrast, a very small positive correlation (r=0.29; P=0.0003) between the URI of ^{11}C-NMSP and that of ^{11}C-CFT in the three subregions was found. Thus, the URI of ^{11}C-NMSP was almost constant, irrespective of that of ^{11}C-CFT in the three subregions. Each average ligand image (Fig. 4), which was made by averaging the URI images of five patients with PD, revealed the apparent tendencies of the three ligands.

To evaluate the more detailed regional differences in the ^{11}C-raclopride and ^{11}C-NMSP binding in the three subregions of the striatum, ratios of the URI of ^{11}C-raclopride to that of ^{11}C-NMSP (R/N ratios) were plotted, as shown in Fig. 5. In normal individuals, the R/N ratios in all three subregions of the striatum were maintained in a constant range. Conversely, in patients with PD, the R/N ratios were significantly higher in the following order: the posterior putamen > anterior putamen > caudate.

Table 2 shows the comparison in the URI of three tracers between the contralateral and ipsilateral sides to the predominant symptoms in patients with PD. For ^{11}C-raclopride, the contralateral URI in all subregions of the striatum tended to be larger than the ipsilateral URI. For both ^{11}C-NMSP and ^{11}C-CFT, the contralateral URI in all subregions of the striatum tended to be smaller than the ipsilateral URI.

Fig. 1

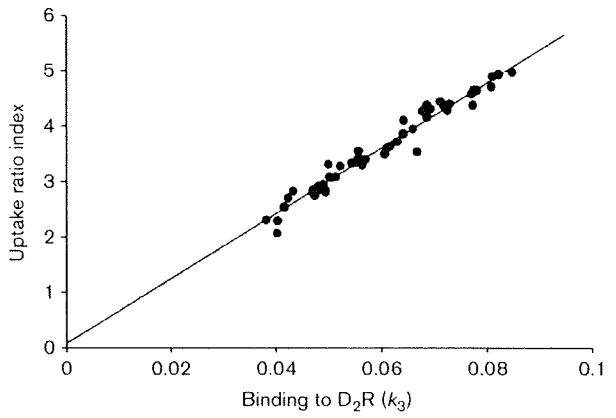

Correlation between the binding to D_2 receptors (D_2R) [association constant (k_3)] and uptake ratio index of ^{11}C-*N*-methylspiperone in the striatum. The solid line represents the regression line. Linear correlation is significant (r=0.98; P<0.0001).

Discussion

In this study, we investigated whether the increase of ^{11}C-raclopride binding in the striatum of patients with PD is associated with the depletion of endogenous dopamine by examining the PET scans of ^{11}C-raclopride, ^{11}C-NMSP, and ^{11}C-CFT in normal individuals and patients with PD.

In normal individuals, earlier neuroimaging studies reported that there was a significant linear correlation between DATs and D_2Rs in the three subregions of the striatum, irrespective of age [3,30]. This study showed

Fig. 2

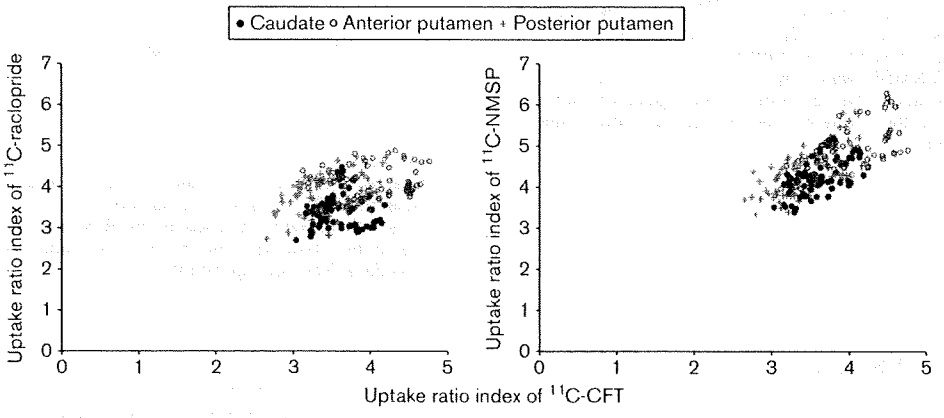

Correlation between the uptake ratio indices of ^{11}C-2β-carbomethoxy-3β-(4-fluorophenyl)-tropane (^{11}C-CFT) and ^{11}C-raclopride (left) and between the uptake ratio indices of ^{11}C-CFT and ^{11}C-*N*-methylspiperone (^{11}C-NMSP) (right) in controls. Closed circles, open circles, and plus signs represent the caudate, anterior putamen, and posterior putamen, respectively. In the graph on the left, a significant correlation is shown only in the posterior putamen (r=0.37, P=0.002). In the graph on the right, there are significant correlations in the caudate (r=0.60, P<0.0001), anterior putamen (r=0.67, P<0.0001), and posterior putamen (r=0.69, P<0.0001).

Fig. 3

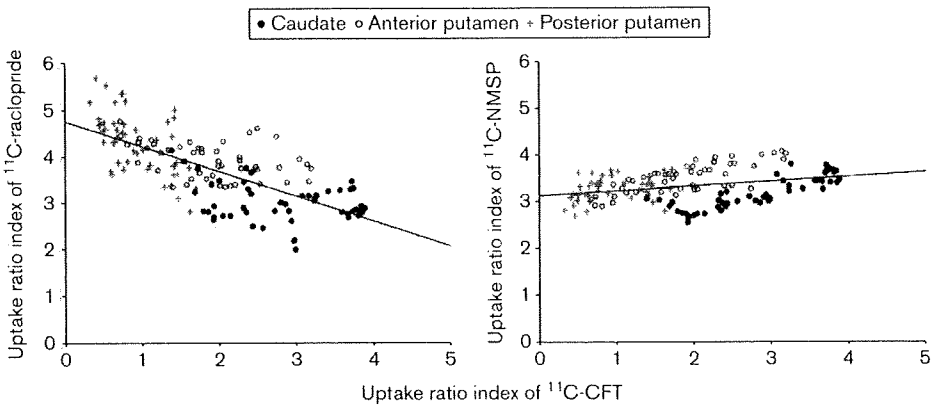

Correlations between the uptake ratio indices of ^{11}C-2β-carbomethoxy-3β-(4-fluorophenyl)-tropane (^{11}C-CFT) and ^{11}C-raclopride (left) and between the uptake ratio indices of ^{11}C-CFT and ^{11}C-*N*-methylspiperone (^{11}C-NMSP) (right) in patients with Parkinson's disease. Closed circles, open circles, and plus signs represent the caudate, anterior putamen, and posterior putamen, respectively. The solid lines represent the regression line for all plots combined with all subregions. Linear correlation is significant in the graph on the left (r=0.71; P<0.0001) and in the graph on the right (r=0.29; P=0.0003).

Fig. 4

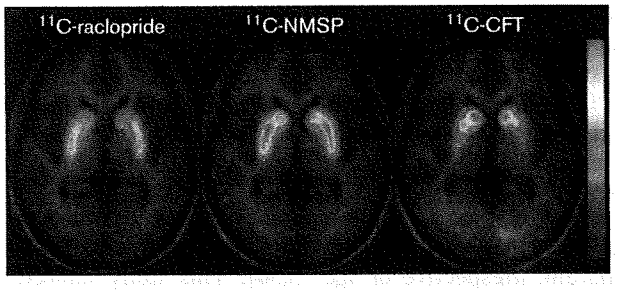

The average ligand images of each tracer superimposed on the average magnetic resonance imaging image at the level of the basal ganglia in patients with Parkinson's disease (PD). Each average ligand image was made by averaging the uptake ratio index images of five patients with PD and clipping the striatum. The binding of ^{11}C-raclopride has an inverse relationship with that of ^{11}C-2β-carbomethoxy-3β-(4-fluorophenyl)-tropane (^{11}C-CFT). The binding of ^{11}C-*N*-methylspiperone (^{11}C-NMSP) was fairly uniform in all subregions of the striatum. For demonstration, the right side of the regions of interest placed on the striatum (the caudate, anterior putamen, and posterior putamen) is displayed.

Fig. 5

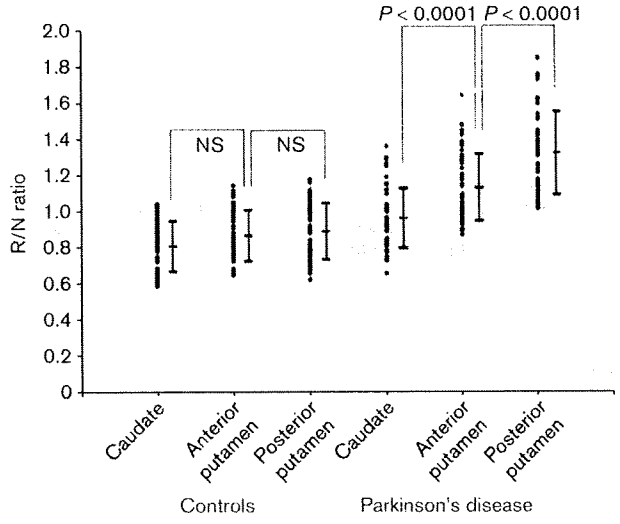

Uptake ratio indices of ^{11}C-raclopride to that of ^{11}C-*N*-methylspiperone (R/N ratios) in the caudate, anterior putamen, and posterior putamen. In controls, the R/N ratios are maintained within a constant range. In patients with Parkinson's disease, the R/N ratios are significantly greater in the following order: the posterior putamen, anterior putamen, and caudate. NS, not significant.

that the URI of ^{11}C-CFT in the three subregions of the striatum was more strongly associated with that of ^{11}C-NMSP than that of ^{11}C-raclopride (Fig. 2). As described in the Introduction, the different binding properties between the two D_2R ligands were considered to be a result of the variability in the binding of ^{11}C-raclopride, in response to changes in the endogenous dopamine concentrations caused by various physiological factors.

Figures 3 and 4 showed that in patients with PD the URI of ^{11}C-raclopride in the three subregions had an inverse relationship with that of ^{11}C-CFT. Morphological and neuroimaging studies for PD have established the following: (i) neuronal loss begins in the lateral ventral nigra, which projects toward the posterior putamen, and throughout the illness this region remains the most severely affected [31,32]. (ii) Severe dopamine depletion was found in the posterior putamen with relative sparing of the caudate nucleus [15]. (iii) DAT levels correlate

the URI of ^{11}C-raclopride in the posterior putamen, in which the presynaptic degeneration occurred most profoundly in the striatum, was relatively higher than that of ^{11}C-NMSP. These findings showed that different concentrations of endogenous dopamine had different effects on the binding properties of the two D_2R ligands. Therefore, we concluded that the increase in ^{11}C-raclopride binding in the striatum of patients with PD is strongly associated with the depletion of endogenous dopamine. ^{11}C-NMSP can be chosen in place of ^{11}C-raclopride in cases in which it may be essential to eliminate the influence of endogenous dopamine.

Acknowledgements

The authors are grateful to Mr Keiichi Kawasaki and Ms Hiroko Tsukinari for their technical assistance and insightful discussions. This study was supported by a Grant-in-Aid for Scientific Research (B) No. 20390334 by the Japan Society for the Promotion of Science (JSPS).

References

1 Farde L, Pauli S, Hall H, Eriksson L, Halldin C, Hogberg T, *et al.* Stereoselective binding of 11C-raclopride in living human brain – a search for extrastriatal central D2-dopamine receptors by PET. *Psychopharmacology (Berl)* 1988; **94**:471–478.

2 Kohler C, Hall H, Ogren SO, Gawell L. Specific in vitro and in vivo binding of 3H-raclopride. A potent substituted benzamide drug with high affinity for dopamine D-2 receptors in the rat brain. *Biochem Pharmacol* 1985; **34**:2251–2259.

3 Ishibashi K, Ishii K, Oda K, Kawasaki K, Mizusawa H, Ishiwata K. Regional analysis of age-related decline in dopamine transporters and dopamine D2-like receptors in human striatum. *Synapse* 2009; **63**:282–290.

4 Hall H, Wedel I, Halldin C, Kopp J, Farde L. Comparison of the in vitro receptor binding properties of N-[3H]methylspiperone and [3H]raclopride to rat and human brain membranes. *J Neurochem* 1990; **55**:2048–2057.

5 Inoue O, Kobayashi K, Tsukada H, Itoh T, Langstrom B. Difference in in vivo receptor binding between [3H]N-methylspiperone and [3H]raclopride in reserpine-treated mouse brain. *J Neural Transm Gen Sect* 1991; **85**:1–10.

6 Young LT, Wong DF, Goldman S, Minkin E, Chen C, Matsumura K, *et al.* Effects of endogenous dopamine on kinetics of [3H]N-methylspiperone and [3H]raclopride binding in the rat brain. *Synapse* 1991; **9**:188–194.

7 Terai M, Hidaka K, Nakamura Y. Comparison of [3H]YM-09151-2 with [3H]spiperone and [3H]raclopride for dopamine d-2 receptor binding to rat striatum. *Eur J Pharmacol* 1989; **173**:177–182.

8 Seeman P, Guan HC, Niznik HB. Endogenous dopamine lowers the dopamine D2 receptor density as measured by [3H]raclopride: implications for positron emission tomography of the human brain. *Synapse* 1989; **3**:96–97.

9 Hall H, Farde L, Sedvall G. Human dopamine receptor subtypes – in vitro binding analysis using 3H-SCH 23390 and 3H-raclopride. *J Neural Transm* 1988; **73**:7–21.

10 Ishibashi K, Kanemaru K, Saito Y, Murayama S, Oda K, Ishiwata K, *et al.* Cerebrospinal fluid metabolite and nigrostriatal dopaminergic function in Parkinson's disease. *Acta Neurol Scand.* (in press).

11 Seeldrayers P, Messina D, Desmedt D, Dalesio O, Hildebrand J. CSF levels of neurotransmitters in Alzheimer-type dementia. Effects of ergoloid mesylate. *Acta Neurol Scand* 1985; **71**:411–414.

12 Hildebrand J, Bourgeois F, Buyse M, Przedborski S, Goldman S. Reproducibility of monoamine metabolite measurements in human cerebrospinal fluid. *Acta Neurol Scand* 1990; **81**:427–430.

13 Guttman M, Seeman P, Reynolds GP, Riederer P, Jellinger K, Tourtellotte WW. Dopamine D2 receptor density remains constant in treated Parkinson's disease. *Ann Neurol* 1986; **19**:487–492.

14 Bokobza B, Ruberg M, Scatton B, Javoy-Agid F, Agid Y. [3H]spiperone binding, dopamine and HVA concentrations in Parkinson's disease and supranuclear palsy. *Eur J Pharmacol* 1984; **99**:167–175.

15 Kish SJ, Shannak K, Hornykiewicz O. Uneven pattern of dopamine loss in the striatum of patients with idiopathic Parkinson's disease. Pathophysiologic and clinical implications. *N Engl J Med* 1988; **318**:876–880.

16 Morrish PK, Sawle GV, Brooks DJ. An [18F]dopa-PET and clinical study of the rate of progression in Parkinson's disease. *Brain* 1996; **119 (Pt 2)**:585–591.

17 Brooks DJ, Ibanez V, Sawle GV, Quinn N, Lees AJ, Mathias CJ, *et al.* Differing patterns of striatal 18F-dopa uptake in Parkinson's disease, multiple system atrophy, and progressive supranuclear palsy. *Ann Neurol* 1990; **28**:547–555.

18 Frost JJ, Rosier AJ, Reich SG, Smith JS, Ehlers MD, Snyder SH, *et al.* Positron emission tomographic imaging of the dopamine transporter with 11C-WIN 35 428 reveals marked declines in mild Parkinson's disease. *Ann Neurol* 1993; **34**:423–431.

19 Nurmi E, Bergman J, Eskola O, Solin O, Vahlberg T, Sonninen P, *et al.* Progression of dopaminergic hypofunction in striatal subregions in Parkinson's disease using [18F]CFT PET. *Synapse* 2003; **48**:109–115.

20 Rinne JO, Ruottinen H, Bergman J, Haaparanta M, Sonninen P, Solin O. Usefulness of a dopamine transporter PET ligand [(18)F]beta-CFT in assessing disability in Parkinson's disease. *J Neurol Neurosurg Psychiatry* 1999; **67**:737–741.

21 Kaasinen V, Ruottinen HM, Nagren K, Lehikoinen P, Oikonen V, Rinne JO. Upregulation of putaminal dopamine D2 receptors in early Parkinson's disease: a comparative PET study with [11C] raclopride and [11C]N-methylspiperone. *J Nucl Med* 2000; **41**:65–70.

22 Hashimoto M, Kawasaki K, Suzuki M, Mitani K, Murayama S, Mishina M, *et al.* Presynaptic and postsynaptic nigrostriatal dopaminergic functions in multiple system atrophy. *Neuroreport* 2008; **19**:145–150.

23 Langer ONK, Dolle F, Lundkvist C, Sandell J, Swahn CG, Vaufrey F, *et al.* Precursor synthesis and radiolabelling of the dopamine D2 receptor ligand [11C]raclopride from [11C]methyl triflate. *J Labelled Comp Radiopharm* 1999; **42**:1183–1193.

24 Kawamura K, Oda K, Ishiwata K. Age-related changes of the [11C]CFT binding to the striatal dopamine transporters in the Fischer 344 rats: a PET study. *Ann Nucl Med* 2003; **17**:249–253.

25 Meyer JH, Gunn RN, Myers R, Grasby PM. Assessment of spatial normalization of PET ligand images using ligand-specific templates. *Neuroimage* 1999; **9**:545–553.

26 Gispert JD, Pascau J, Reig S, Martinez-Lazaro R, Molina V, Garcia-Barreno P, *et al.* Influence of the normalization template on the outcome of statistical parametric mapping of PET scans. *Neuroimage* 2003; **19**:601–612.

27 Antonini A, Leenders KL, Reist H, Thomann R, Beer HF, Locher J. Effect of age on D2 dopamine receptors in normal human brain measured by positron emission tomography and 11C-raclopride. *Arch Neurol* 1993; **50**:474–480.

28 Wong DF, Wagner HN Jr, Dannals RF, Links JM, Frost JJ, Ravert HT, *et al.* Effects of age on dopamine and serotonin receptors measured by positron tomography in the living human brain. *Science* 1984; **226**: 1393–1396.

29 Hagglund J, Aquilonius SM, Eckernas SA, Hartvig P, Lundquist H, Gullberg P, *et al.* Dopamine receptor properties in Parkinson's disease and Huntington's chorea evaluated by positron emission tomography using 11C-N-methylspiperone. *Acta Neurol Scand* 1987; **75**:87–94.

30 Volkow ND, Wang GJ, Fowler JS, Ding YS, Gur RC, Gatley J, *et al.* Parallel loss of presynaptic and postsynaptic dopamine markers in normal aging. *Ann Neurol* 1998; **44**:143–147.

31 Gibb WR, Lees AJ. Anatomy, pigmentation, ventral and dorsal subpopulations of the substantia nigra, and differential cell death in Parkinson's disease. *J Neurol Neurosurg Psychiatry* 1991; **54**:388–396.

32 Fearnley JM, Lees AJ. Ageing and Parkinson's disease: substantia nigra regional selectivity. *Brain* 1991; **114 (Pt 5)**:2283–2301.

33 Bezard E, Dovero S, Prunier C, Ravenscroft P, Chalon S, Guilloteau D, *et al.* Relationship between the appearance of symptoms and the level of nigrostriatal degeneration in a progressive 1-methyl-4-phenyl-1,2,3,6-tetrahydropyridine-lesioned macaque model of Parkinson's disease. *J Neurosci* 2001; **21**:6853–6861.

34 Dewey SL, Smith GS, Logan J, Brodie JD, Fowler JS, Wolf AP. Striatal binding of the PET ligand 11C-raclopride is altered by drugs that modify synaptic dopamine levels. *Synapse* 1993; **13**:350–356.

35 Ishiwata K, Hayakawa N, Ogi N, Oda K, Toyama H, Endo K, *et al.* Comparison of three PET dopamine D2-like receptor ligands, [11C]raclopride, [11C]nemonapride and [11C]N-methylspiperone, in rats. *Ann Nucl Med* 1999; **13**:161–167.

36 Seeman P, Niznik HB, Guan HC. Elevation of dopamine D2 receptors in schizophrenia is underestimated by radioactive raclopride. *Arch Gen Psychiatry* 1990; **47**:1170–1172.

the URI of ^{11}C-raclopride in the posterior putamen, in which the presynaptic degeneration occurred most profoundly in the striatum, was relatively higher than that of ^{11}C-NMSP. These findings showed that different concentrations of endogenous dopamine had different effects on the binding properties of the two D_2R ligands. Therefore, we concluded that the increase in ^{11}C-raclopride binding in the striatum of patients with PD is strongly associated with the depletion of endogenous dopamine. ^{11}C-NMSP can be chosen in place of ^{11}C-raclopride in cases in which it may be essential to eliminate the influence of endogenous dopamine.

Acknowledgements

The authors are grateful to Mr Keiichi Kawasaki and Ms Hiroko Tsukinari for their technical assistance and insightful discussions. This study was supported by a Grant-in-Aid for Scientific Research (B) No. 20390334 by the Japan Society for the Promotion of Science (JSPS).

References

1 Farde L, Pauli S, Hall H, Eriksson L, Halldin C, Hogberg T, *et al.* Stereoselective binding of 11C-raclopride in living human brain – a search for extrastriatal central D2-dopamine receptors by PET. *Psychopharmacology (Berl)* 1988; **94**:471–478.

2 Kohler C, Hall H, Ogren SO, Gawell L. Specific in vitro and in vivo binding of 3H-raclopride. A potent substituted benzamide drug with high affinity for dopamine D-2 receptors in the rat brain. *Biochem Pharmacol* 1985; **34**:2251–2259.

3 Ishibashi K, Ishii K, Oda K, Kawasaki K, Mizusawa H, Ishiwata K. Regional analysis of age-related decline in dopamine transporters and dopamine D2-like receptors in human striatum. *Synapse* 2009; **63**:282–290.

4 Hall H, Wedel I, Halldin C, Kopp J, Farde L. Comparison of the in vitro receptor binding properties of N-[3H]methylspiperone and [3H]raclopride to rat and human brain membranes. *J Neurochem* 1990; **55**:2048–2057.

5 Inoue O, Kobayashi K, Tsukada H, Itoh T, Langstrom B. Difference in in vivo receptor binding between [3H]N-methylspiperone and [3H]raclopride in reserpine-treated mouse brain. *J Neural Transm Gen Sect* 1991; **85**:1–10.

6 Young LT, Wong DF, Goldman S, Minkin E, Chen C, Matsumura K, *et al.* Effects of endogenous dopamine on kinetics of [3H]N-methylspiperone and [3H]raclopride binding in the rat brain. *Synapse* 1991; **9**:188–194.

7 Terai M, Hidaka K, Nakamura Y. Comparison of [3H]YM-09151-2 with [3H]spiperone and [3H]raclopride for dopamine d-2 receptor binding to rat striatum. *Eur J Pharmacol* 1989; **173**:177–182.

8 Seeman P, Guan HC, Niznik HB. Endogenous dopamine lowers the dopamine D2 receptor density as measured by [3H]raclopride: implications for positron emission tomography of the human brain. *Synapse* 1989; **3**:96–97.

9 Hall H, Farde L, Sedvall G. Human dopamine receptor subtypes – in vitro binding analysis using 3H-SCH 23390 and 3H-raclopride. *J Neural Transm* 1988; **73**:7–21.

10 Ishibashi K, Kanemaru K, Saito Y, Murayama S, Oda K, Ishiwata K, *et al.* Cerebrospinal fluid metabolite and nigrostriatal dopaminergic function in Parkinson's disease. *Acta Neurol Scand.* (in press).

11 Seeldrayers P, Messina D, Desmedt D, Dalesio O, Hildebrand J. CSF levels of neurotransmitters in Alzheimer-type dementia. Effects of ergoloid mesylate. *Acta Neurol Scand* 1985; **71**:411–414.

12 Hildebrand J, Bourgeois F, Buyse M, Przedborski S, Goldman S. Reproducibility of monoamine metabolite measurements in human cerebrospinal fluid. *Acta Neurol Scand* 1990; **81**:427–430.

13 Guttman M, Seeman P, Reynolds GP, Riederer P, Jellinger K, Tourtellotte WW. Dopamine D2 receptor density remains constant in treated Parkinson's disease. *Ann Neurol* 1986; **19**:487–492.

14 Bokobza B, Ruberg M, Scatton B, Javoy-Agid F, Agid Y. [3H]spiperone binding, dopamine and HVA concentrations in Parkinson's disease and supranuclear palsy. *Eur J Pharmacol* 1984; **99**:167–175.

15 Kish SJ, Shannak K, Hornykiewicz O. Uneven pattern of dopamine loss in the striatum of patients with idiopathic Parkinson's disease. Pathophysiologic and clinical implications. *N Engl J Med* 1988; **318**:876–880.

16 Morrish PK, Sawle GV, Brooks DJ. An [18F]dopa-PET and clinical study of the rate of progression in Parkinson's disease. *Brain* 1996; **119 (Pt 2)**:585–591.

17 Brooks DJ, Ibanez V, Sawle GV, Quinn N, Lees AJ, Mathias CJ, *et al.* Differing patterns of striatal 18F-dopa uptake in Parkinson's disease, multiple system atrophy, and progressive supranuclear palsy. *Ann Neurol* 1990; **28**:547–555.

18 Frost JJ, Rosier AJ, Reich SG, Smith JS, Ehlers MD, Snyder SH, *et al.* Positron emission tomographic imaging of the dopamine transporter with 11C-WIN 35 428 reveals marked declines in mild Parkinson's disease. *Ann Neurol* 1993; **34**:423–431.

19 Nurmi E, Bergman J, Eskola O, Solin O, Vahlberg T, Sonninen P, *et al.* Progression of dopaminergic hypofunction in striatal subregions in Parkinson's disease using [18F]CFT PET. *Synapse* 2003; **48**:109–115.

20 Rinne JO, Ruottinen H, Bergman J, Haaparanta M, Sonninen P, Solin O. Usefulness of a dopamine transporter PET ligand [(18)F]beta-CFT in assessing disability in Parkinson's disease. *J Neurol Neurosurg Psychiatry* 1999; **67**:737–741.

21 Kaasinen V, Ruottinen HM, Nagren K, Lehikoinen P, Oikonen V, Rinne JO. Upregulation of putaminal dopamine D2 receptors in early Parkinson's disease: a comparative PET study with [11C] raclopride and [11C]N-methylspiperone. *J Nucl Med* 2000; **41**:65–70.

22 Hashimoto M, Kawasaki K, Suzuki M, Mitani K, Murayama S, Mishina M, *et al.* Presynaptic and postsynaptic nigrostriatal dopaminergic functions in multiple system atrophy. *Neuroreport* 2008; **19**:145–150.

23 Langer ONK, Dolle F, Lundkvist C, Sandell J, Swahn CG, Vaufrey F, *et al.* Precursor synthesis and radiolabelling of the dopamine D2 receptor ligand [11C]raclopride from [11C]methyl triflate. *J Labelled Comp Radiopharm* 1999; **42**:1183–1193.

24 Kawamura K, Oda K, Ishiwata K. Age-related changes of the [11C]CFT binding to the striatal dopamine transporters in the Fischer 344 rats: a PET study. *Ann Nucl Med* 2003; **17**:249–253.

25 Meyer JH, Gunn RN, Myers R, Grasby PM. Assessment of spatial normalization of PET ligand images using ligand-specific templates. *Neuroimage* 1999; **9**:545–553.

26 Gispert JD, Pascau J, Reig S, Martinez-Lazaro R, Molina V, Garcia-Barreno P, *et al.* Influence of the normalization template on the outcome of statistical parametric mapping of PET scans. *Neuroimage* 2003; **19**:601–612.

27 Antonini A, Leenders KL, Reist H, Thomann R, Beer HF, Locher J. Effect of age on D2 dopamine receptors in normal human brain measured by positron emission tomography and 11C-raclopride. *Arch Neurol* 1993; **50**:474–480.

28 Wong DF, Wagner HN Jr, Dannals RF, Links JM, Frost JJ, Ravert HT, *et al.* Effects of age on dopamine and serotonin receptors measured by positron tomography in the living human brain. *Science* 1984; **226**: 1393–1396.

29 Hagglund J, Aquilonius SM, Eckernas SA, Hartvig P, Lundquist H, Gullberg P, *et al.* Dopamine receptor properties in Parkinson's disease and Huntington's chorea evaluated by positron emission tomography using 11C-N-methyl-spiperone. *Acta Neurol Scand* 1987; **75**:87–94.

30 Volkow ND, Wang GJ, Fowler JS, Ding YS, Gur RC, Gatley J, *et al.* Parallel loss of presynaptic and postsynaptic dopamine markers in normal aging. *Ann Neurol* 1998; **44**:143–147.

31 Gibb WR, Lees AJ. Anatomy, pigmentation, ventral and dorsal subpopulations of the substantia nigra, and differential cell death in Parkinson's disease. *J Neurol Neurosurg Psychiatry* 1991; **54**:388–396.

32 Fearnley JM, Lees AJ. Ageing and Parkinson's disease: substantia nigra regional selectivity. *Brain* 1991; **114 (Pt 5)**:2283–2301.

33 Bezard E, Dovero S, Prunier C, Ravenscroft P, Chalon S, Guilloteau D, *et al.* Relationship between the appearance of symptoms and the level of nigrostriatal degeneration in a progressive 1-methyl-4-phenyl-1,2,3,6-tetrahydropyridine-lesioned macaque model of Parkinson's disease. *J Neurosci* 2001; **21**:6853–6861.

34 Dewey SL, Smith GS, Logan J, Brodie JD, Fowler JS, Wolf AP. Striatal binding of the PET ligand 11C-raclopride is altered by drugs that modify synaptic dopamine levels. *Synapse* 1993; **13**:350–356.

35 Ishiwata K, Hayakawa N, Ogi N, Oda K, Toyama H, Endo K, *et al.* Comparison of three PET dopamine D2-like receptor ligands, [11C]raclopride, [11C]nemonapride and [11C]N-methylspiperone, in rats. *Ann Nucl Med* 1999; **13**:161–167.

36 Seeman P, Niznik HB, Guan HC. Elevation of dopamine D2 receptors in schizophrenia is underestimated by radioactive raclopride. *Arch Gen Psychiatry* 1990; **47**:1170–1172.

37 Antonini A, Schwarz J, Oertel WH, Beer HF, Madeja UD, Leenders KL. [11C]raclopride and positron emission tomography in previously untreated patients with Parkinson's disease: Influence of L-dopa and lisuride therapy on striatal dopamine D2-receptors. *Neurology* 1994; **44**:1325–1329.

38 Rinne JO, Laihinen A, Rinne UK, Nagren K, Bergman J, Ruotsalainen U. PET study on striatal dopamine D2 receptor changes during the progression of early Parkinson's disease. *Mov Disord* 1993; **8**:134–138.

39 Sawle GV, Playford ED, Brooks DJ, Quinn N, Frackowiak RS. Asymmetrical pre-synaptic and post-synpatic changes in the striatal dopamine projection in dopa naive parkinsonism. Diagnostic implications of the D2 receptor status. *Brain* 1993; **116 (Pt 4)**:853–867.

40 Rutgers AW, Lakke JP, Paans AM, Vaalburg W, Korf J. Tracing of dopamine receptors in hemiparkinsonism with positron emission tomography (PET). *J Neurol Sci* 1987; **80**:237–248.

Movement Disorders
Vol. 00. No. 00, 2009, pp. 000–000

Photophobia in Essential Blepharospasm—A Positron Emission Tomographic Study

Hirofumi Emoto, MD,[1,2] Yukihisa Suzuki,[1,2] Masato Wakakura,[3] Chiharu Horie,[1,2] Motohiro Kiyosawa,[2] Manabu Mochizuki,[2] Keiichi Kawasaki,[1] Keiichi Oda,[1] Kiichi Ishiwata,[1] and Kenji Ishii[1]*

[1]*Positron Medical Center, Tokyo Metropolitan Institute of Gerontology, Tokyo, Japan*
[2]*Department of Ophthalmology and Visual Science, Tokyo Medical and Dental University, Graduate School of Medical and Dental Sciences, Tokyo, Japan*
[3]*Department of Neuro-Ophthalmology, Inouye Eye Hospital, Tokyo, Japan*

Abstract: To localize regional alterations in cerebral glucose metabolism in essential blepharospasm (EB) patients with photophobia. We have studied 22 EB patients by performing positron emission tomography and [^{18}F]-fluorodeoxyglucose analysis. The patients were classified into two subgroups, namely, EB with photophobia (P group) and EB without photophobia (NP group), and compared with a healthy control group (n = 44). There were no significant differences between the two patient groups with respect to the severity of motor symptoms or the duration for which the condition persisted. The FDG-PET images were analyzed using the statistical parametric mapping software. As compared to the control group, the P group exhibited significant hypermetabolism in the thalamus (P = 0.002), while the NP group exhibited significant hypometabolism in the dorsal midbrain, especially, in the superior colliculus (P = 0.005). The P group exhibited significant hypermetabolism in the thalamus and the dorsal midbrain as compared to the NP group ($P <$ 0.001). These findings suggest that photophobia in EB patients may be associated with abnormal hyperactivity in the thalamus. Either hyperactivity of the thalamus or hypoactivity of the superior colliculus, or both may be associated with excessive blinking in these patients. © 2009 Movement Disorder Society

Key words: photophobia; essential blepharospasm; positron emission tomography; thalamus; superior colliculus

INTRODUCTION

Photophobia in Essential Blepharospasm

Essential blepharospasm (EB) is a form of common focal dystonia that is characterized by involuntary forceful contraction of the eyelid protractor.[1] The etiology of this condition remains obscure, but there are several reports of the formation of lesions in the basal ganglia, thalamus, and brainstem in EB patients.[1–3] In addition to the motor symptom of eyelid spasm, patients with EB frequently complain of photophobia, a sensory symptom, which precedes or occurs simultaneously with the development of eyelid spasms.[4,5] Many EB patients wear sunglasses even on cloudy days, as daylight causes ocular discomfort.[6,7] In a survey, 79% of 1,653 EB patients reported that bright light was the most frequent exacerbating factor and worsened their eyelid spasms.[8] Photophobia in EB patients is a complex symptom associated with pain or discomfort in the eyes and appears to be the reason why light aggravates eyelid spasms.[1] Even after the muscle spasm is relieved, bright light still bothers these patients.[4–6] The photophobia in EB can be reduced significantly by photochromatic modulation with specially tinted lenses.[7] Furthermore, aggressive treatment of dry eye syndrome can often ameliorate eye pain or discomfort of EB.

Mechanism of Photophobia

Photophobia is common in patients with disorders of the iris and anterior segment of the eye, such as exposure

Presented in part at the 10th International Congress of Parkinson's Disease and Movement Disorders, 2006, Kyoto, Japan, and the 16th International Neuro-Ophthalmology Society Meeting, 2006, Tokyo, Japan.
*Correspondence to: Kenji Ishii, Positron Medical Center, Tokyo Metropolitan Institute of Gerontology, 1-1 Naka-cho, Itabashi-ku, Tokyo 173-0022, Japan. E-mail: ishii@pet.tmig.or.jp
Potential conflict of interest: Nothing to report.
Received 16 November 2008; Revised 1 October 2009; Accepted 30 October 2009
Published online in Wiley InterScience(www.interscience. wiley.com). DOI: 10.1002/mds.22916

keratitis (secondary to blepharospasm). It has also been reported in conditions, wherein the anterior segment of the eye appears normal, including migraine, meningitis, and subarachnoid hemorrhage.[1] Most of the published reports on EB have focused on the motor signs, and little attention has been paid to photophobia. The mechanism of photophobia is not completely understood, but is thought to involve the trigeminal pathway, with possible inputs from the occipital lobe and thalamus.[1] Adams et al.[9] postulated the trigeminal pathway and thalamus mediate the symptoms of photophobia in EB and Burstein et al.[10] did so in migraine. It has also been postulated that photophobia in EB may represent a form of sympathetically maintained pain disorder and some patients experienced relief from superior cervical ganglion blocks.[6] Among the parts of the brain that have been proposed to be associated with EB, the thalamus is the major part that transmits various afferent signals, such as visual, auditory, and somatosensory (including trigeminal) signals to the cerebral and the cerebellar cortices.[11] The thalamus plays an important role in dystonia subjects,[12] and the results of our previous study suggested that altered neural activities in the thalamus may be essential for the development of EB.[2] On the other hand, the brainstem comprises cranial nerves that are also associated with the transmission of signals for vision, pain, and trigeminal blink reflex. The superior colliculus is an anatomically and physiologically complex structure involved in multimodal sensorimotor functions,[13,14] and the pretectal area is associated with light reflexes.[15]

We hypothesized that the lesions attributable to photophobia in EB are formed in the thalamus or brainstem. We used positron emission tomography with [^{18}F]-fluorodeoxyglucose (FDG-PET) to localize the regional alterations in cerebral glucose metabolism in EB patients with photophobia.

We compared the FDG-PET images of EB patients with and without photophobia and control subjects. Previous FDG-PET studies have demonstrated that in EB patients, glucose metabolism is altered in the thalamus[2,16] and cerebellum.[17] However, there have been few studies on the functional neuroimaging of sensorimotor processing in patients with EB or focal dystonia.[1] To our knowledge, this is the first PET study on photophobia in EB.

PATIENTS AND METHODS

Patients

The patients with bilateral EB were recruited from the Outpatient Department of the Inouye Eye Hospital and provide informed consent. Medical history and a questionnaire of these subjects were recorded to obtain relevant information about photophobia. The photophobia was assessed using the rating scale; 0: none, 1: mild, 2: moderate, and 3: severe (1: the patients reported they had photophobia but it was minimum, 2: the photophobia was not minimum, but it was not too severe to affect their quality of life, 3: the photophobia hampered their quality of life). We did not measure a threshold for light sensitivity in these patients.[9]

In total, 82 patients with EB were enrolled in this study. Of 82 patients, there were 11 EB patients rating as 0 in photophobia (i.e. EB without photophobia) and they were classified as NP group (n = 11, M = 2, F = 9; average age: 53.3 years, range: 30–64 years). Of 71 patients with EB had photophobia to some extent, we selected age- and gender-matched 11 patients rating as three in photophobia (i.e. EB with severe photophobia) consecutively, and they were classified as P group (n = 11, M = 2, F = 9; average age: 47.5 years, range: 28–60 years). The severity of blepharospasm was assessed according to the criteria of Jankovic[18] (Table 1). There was no significant difference between the two patient groups with respect to the severity of motor symptoms or the duration, for which the condition persisted. The subjects had undergone magnetic resonance imaging (MRI) and FDG-PET scanning at the Positron Medical Center, Tokyo Metropolitan Institute of Gerontology. None of the patients and controls had any other neuropsychiatric disorders or organic lesions in the brain, as revealed by MRI, or had been administered any psychotropic drugs for at least 2 weeks before the study began. Written informed consent was obtained from all subjects after the purpose and procedures of the experiments including MRI and PET were thoroughly explained before participation in the study. This study was approved by the institutional ethics committee.

PET Data Acquisition

PET scans were performed using the SET 2400 W scanner (Shimadzu, Kyoto, Japan) at the Positron Medical Center, Tokyo Metropolitan Institute of Gerontology. Attenuation was corrected by transmission scanning with a ^{68}Ga/^{68}Ge rotating source. Arterial blood sampling was not performed, and thus the images acquired were those of tissue activity. For FDG-PET scanning, a bolus of 120 MBq FDG was injected intravenously, and the patients were requested to lie comfortably with their eyes closed. A 6-min emission scan in the 3D acquisition mode was obtained 45 min after

TABLE 1. *Demographic data of the P group, NP group, and controls*

	P group	NP group	controls
Males:Females	2:9	2:9	2:9
Average age in yr (range)	47.5 (28–60)	55.3 (30–64)	52.7 (25–67)
Average months since the onset of EB (range)	29.1 (7–84)	38.5 (1–120)	–
Average number of months since last injection of botulinum toxin (range)	2.3 (1–5)	2.0 (0–4)	–
Severity of blepharospasm*	None: 0	None: 0	–
	Noticeable: 0	Noticeable: 0	
	Mild: 2	Mild: 2	
	Moderate: 7	Moderate: 6	
	Severe: 2	Severe: 3	

*There was no dominant side. Severity of EB in patients was assessed using the rating scale developed by Jankovic: 0; none, 1; noticeable, 2; mild, 3; moderate, 4; severe.

the injection. We obtained 50 transaxial images at an interslice interval of 3.125 min. The spatial resolution of the reconstructed images was 6 × 6 × 7.5 mm full-width half-maximum (FWHM). The MR images were obtained by using a 1.5T scanner (Signa Excite; GE, Milwaukee, WI, USA), and each subject underwent a routine brain diagnostic scan along with 3D spoiled gradient recalled (3DSPGR) scan (TR = 9.2 ms, TE = 2.0 ms, matrix size = 256 × 256 × 124, voxel size = 0.94 × 0.94 × 1.3 mm) to provide anatomical reference data for PET.

Data Processing and Statistical Analysis

The PET images were coregistered with 3DSPGR images using the Automated Medical Images Registration (AMIR) program. The PET image of each subject was transformed into the standard anatomical space defined by the Montreal Neurological Institute (MNI) by using an in-house FDG template, and the same transformation matrix was applied to the corresponding MR images to obtain individual FDG-matched MRI images in the MNI space. After the anatomical standardization, all PET images were smoothed using a Gaussian filter (16 mm FWHM). The preprocessing and statistical analysis of these images were performed using the statistical parametric mapping program (SPM2; Wellcome Department of Imaging Neuroscience, Institute of Neurology, London, UK) that was implemented in Matlab (Mathworks, Sherborn, MA, USA).

Statistical parametric maps were created by combining the general linear model and the theory of Gaussian fields to form statistical inferences regarding the regional effects. After the appropriate design matrix was specified using the proportional scaling for global normalization, the differences between the groups were estimated by performing an analysis of covariance (ANCOVA) at every voxel using age as a nuisance covariate. To test the hypotheses regarding the differences in the regional metabolic activity for each group, the estimates were compared using linear contrast. We excluded small areas of regional metabolism alterations (extent threshold, k = 300 voxels). All the regions were classified as being hyper- or hypometabolic, and values that exceeded $P < 0.05$, after correction for cluster level, were considered statistically significant. The resulting sets of voxel values obtained for each contrast constituted a statistical parametric map of the t statistic SPM (t).

The statistical significance of each region was estimated using the distributional approximations on the basis of the theory of Gaussian fields.

MRI-referenced regions of interest (ROIs) were aligned with individual PET images of all subjects with 1-cm-diameter circles to evaluate the distribution patterns of individual regional metabolic level, in terms of the relative FDG uptake in the thalamus and superior colliculus in each group, after the global mean was normalized to 50 by using the Mann-Whitney U test.

RESULTS

Comparison of Results of the Patient Groups and the Control Group

Compared to the control group, the P group exhibited hypermetabolism in the thalamus ($P = 0.034$, corrected for cluster level; Fig. 1A). It included both ventral and anterior portions, but the right side of the thalamus showed predominant hypermetabolism. Both pulvinar regions were included; however, the main hypermetabolic region was located in the ventral anterior nuclei (VA) and the ventral lateral nuclei (VL) of the thalamus. Hypometabolism observed in the thalamus of the P group was not significant when compared to that in the control group.

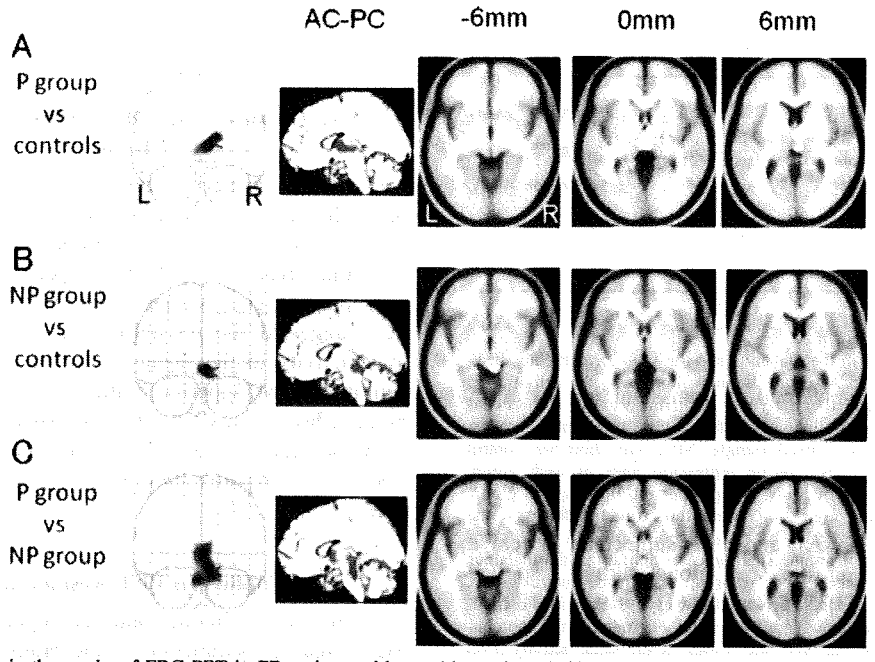

FIG. 1. Difference in the results of FDG-PET in EB patients with or without photophobia. The statistical parametric map results obtained from comparisons between the different groups using the FDG-PET images. A: The contrast P group minus control group shows hypermetabolism in the thalamus ($P = 0.034$, corrected for cluster level). The main hypermetabolic portions in the P group were VA and VL of the thalamus. B: The contrast NP group minus control group shows hypometabolism in the dorsal midbrain ($P = 0.007$, corrected for cluster level). The main hypometabolic area in the NP group was the superior colliculus. C: The contrast P group minus NP group shows that the P group exhibited hypermetabolism in the thalamus and the dorsal midbrain ($P < 0.001$, corrected for cluster level). The main hypermetabolic areas are VA, VL, and superior colliculus.

The NP group exhibited hypometabolism in the dorsal midbrain ($P = 0.007$, corrected for cluster level; Fig. 1B) as compared to the control group. The predominant hypometabolic area was found on the superior colliculus. As compared to the control group, the hypermetabolism in the NP group was not significant.

Comparison of Results of the P Group and the NP Group

Compared to the NP group, the P group exhibited relatively higher hypermetabolism in the thalamus and dorsal midbrain ($P < 0.001$, corrected for cluster level; Fig. 1C). The main hypermetabolic areas in the P group were the VA, VL, and superior colliculus. However, there were no significant hypometabolic areas in the P group as compared to the NP group.

ROI Analysis

Using the Mann-Whitney U test, we compared the results of the ROI analysis (Fig. 2) and found that glucose metabolism in the thalamus in the P group was significantly higher than that in the control and the NP groups ($P < 0.001$; $P < 0.001$, respectively), while the thalamic metabolism in the NP group was significantly lower than in the control group ($P < 0.05$). The glucose metabolism in the superior colliculus was significantly lower in the NP group than in the P and control groups ($P < 0.001$; $P < 0.001$, respectively), while there was no significant difference in the metabolic activity in the superior colliculus between the P and control groups.

In both the P and NP groups, the ratio of the metabolic activity in the superior colliculus to that in the thalamus was significantly lower than the ratio in the control group ($P < 0.005$; $P < 0.005$, respectively), while there was no significant difference between the P and NP groups.

DISCUSSION

Photophobia and the Thalamus

It has been postulated that visual processing occurs via two pathways that work in parallel, namely,the retinogeniculostriate pathway (the primary visual pathway)

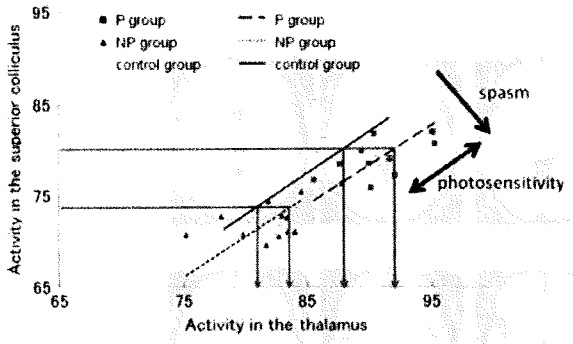

FIG. 2. The activity in the thalamus and the superior colliculus in P, NP, and control group A scatter diagram illustrating the activities of individual regions (global activity was normalized to 50) in the thalamus and the superior colliculus of the P, NP, and control groups. Closed square: P group, closed triangle: NP group, short bar: control group. Three black lines indicate regression lines of each group; dashed line: P group, dotted line: NP group, solid line: control group. Slopes of these three regression lines were similar. However, the regression lines of the P and NP group were shifted to right, compared to that of control group. This indicates activity in the thalamus tends to be higher in the P and NP group than in the control group. The red line shows, at the same activity level in the superior colliculus, activity in the thalamus is higher in the P group than in the control group. Similarly, the blue line shows, at the same activity level in the superior colliculus, activity in the thalamus is higher in the NP group than in the control group. The regression line of NP group was shifted below, compared to those of the P and control group. This indicates activity in the superior colliculus tends to be lower in the NP group than in the P and control group.

and the extrageniculate pathway (the secondary visual pathway). The extrageniculate pathway includes, the retinotectal pathway (mediates orienting response), the retinopretectal pathway (mediates pupillary response), and the retinohypothalamic pathway (related to circadian rhythms). The visual processing in the thalamus is mediated by the lateral geniculate nucleus and the pulvinar via these pathways. The lateral geniculate nucleus is associated with the primary visual pathway, which mediates the conscious visual perception and fine visual recognition. The pulvinar is associated with the secondary visual pathway, which mediates unconscious visual perception such as blindsight. The retinotectal pathway transmits visual signals from the retina to the superior colliculus, and this signal is further transmitted to the pulvinar in the thalamus (tectopulvinar pathway). The medial and lateral pulvinar transmits this information to the parietal and temporal lobes of the brain, respectively. Vision achieved via this pathway has low resolution although it is sensitive to luminance and movement. In our study, as compared to the control and NP group, the P group showed hypermetabolism in both left and right medial pulvinar regions, and hyperactivity in these regions may cause the hypersensitivity to luminance in EB patients with photophobia.

Two Pathways that Modify the Blink Reflex Circuits

Our PET results suggested that EB patients with photophobia show abnormal hyperactivity in the thalamus, whereas EB patients without photophobia show abnormal hypoactivity in the superior colliculus. The neurophysiological studies conducted by microstimulation suggested the possibility that both the abnormal hyperactivity in the thalamus and the abnormal hypoactivity in the superior colliculus could enhance the blink reflex circuits[19–21] (Fig. 3). This is in accordance with the reports that indicate the association between EB and hyperexcitability of trigeminal blink reflex.[22,23]

Conflict in PET Results in EB

There are conflicting data and reports regarding the exact area of dysfunction in the brain in EB.[16] In EB and other dystonias, some reported hypermetabolism in the thalamus and the basal ganglia with FDG-PET.[2,24–26] But Kerrison et al.[27] also reported the thalamus was hypometabolic in EB. Hutchinson et al.[17] reported they predicted the thalamus was hypermetabolic but it was not. Many patients with EB present

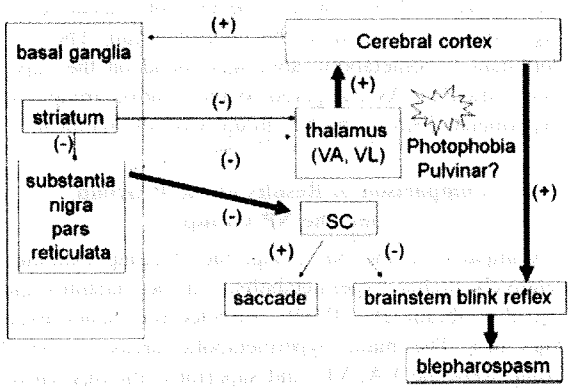

FIG. 3. Neural network model for blepharospasm[19–21] (−), inhibitory pathway; (+), excitatory pathway; solid arrow, enhanced activity; dotted arrow, attenuated activity; SC, superior colliculus; VA, ventral anterior nucleus; VL, ventral lateral nucleus. Abnormally reduced inhibitory signals from the substantia nigra to the excitatory neurons in the thalamus could induce thalamic hyperactivity that could in turn enhance blink reflex circuits via the inputs from the cerebral motor cortex. On the other hand, abnormally increased inhibitory signals from the substantia nigra to inhibitory neurons in the superior colliculus could cause decreased inhibition to the blink reflex circuits, leading to excessive blinking.

photophobia, so PET of those may show hypermetabolism in the thalamus, as seen in the P group. But some patients with EB may not show hypermetabolism in the thalamus, as seen in the NP group (Fig. 1).

Activity Balance Between Thalamus and Superior Colliculus

In the ROI analysis, we examined the activity balance between the thalamus and the superior colliculus (Fig. 2).

Slopes of regression lines of each group were similar. However, the regression lines of the P and NP group were shifted to right, compared to that of control group. This indicates activity in the thalamus tends to be higher in the P and NP group than in the control group. By the Mann-Whitney U test, the activity ratio of the superior colliculus/the thalamus in the P group was significantly less than that in the control group ($P = 0.0031$), while the ratios were not significantly different between two patient groups.

In the NP group, the activity ratio was also significantly less than that in the control group, although the thalamic activities were significantly lower than that in the control group ($P = 0.00294$, $P = 0.00363$, respectively). This suggests that, in the NP group, the activity was relatively higher in the thalamus than in the superior colliculus. This abnormally high activity in the thalamus in both patient groups may be attributable to EB.

In conclusion, we found abnormal hyperactivity in the thalamus in EB patients with photophobia and abnormal hypoactivity in the superior colliculus in EB patients without photophobia by using FDG-PET. Both the conditions indicated that abnormally high activity in the thalamus causes an imbalance between the activities of the superior colliculus and thalamus, and that such an imbalance may induce excessive blinking and blepharospasm. The hyperactivity of the thalamus may also be associated with the symptom of photophobia. Further studies are required to elucidate the specific neural mechanisms involved in the hyperactivity of the thalamus that cause photophobia in EB patients.

Acknowledgments: This work was supported by a Grant-in-Aid for Young Scientists (B) (18991310) from the Ministry for Education, Culture, Sports, Science, and Technology, Japan, by the Grant-in-Aid for Scientific Research (B), No. 20390334 from the Japan Society for the Promotion of Science(Ki.I.), and by the Program for Promotion of Fundamental Studies in Health Sciences of the National Institute of Biomedical Innovation,Japan (No: 06-46, Ki.I.).

Financial Disclosure: The authors have no proprietary interest in any of the material used in this study.

Author Roles: *Hirofumi Emoto*: 1) Research project: Conception, Organization, Execution; Statistical Analysis: Design, Execution, Review and Critique; Manuscript: Writing of the first draft. *Yukihisa Suzuki*: Research project: Conception, Organization, Execution; Statistical Analysis: Review and Critique; Manuscript: Review and Critique. *Masato Wakakura*: Research project: Conception, Organization, Execution; Statistical Analysis: Review and Critique; Manuscript: Review and Critique. *Chiharu Horie*: Research project: Conception, Organization, Execution; Statistical Analysis: Review and Critique; Manuscript: Review and Critique. *Motohiro Kiyosawa*: Research project: Conception, Organization, Execution; Statistical Analysis: Review and Critique; Manuscript: Review and Critique. *Manabu Mochizuki*: Research project: Conception; Review and Critique; Manuscript: Review and Critique. *Keiichi Kawasaki*: Research project: Organization; Review and Critique; Manuscript: Review and Critique. *Keiichi Oda*: Research project: Organization; Review and Critique; Manuscript: Review and Critique. *Kiichi Ishiwata*: Research project: Conception, Organization, Execution; Statistical Analysis: Review and Critique; Manuscript: Review and Critique. *Kenji Ishii*: Research project: Conception, Organization; Statistical Analysis: Design, Execution, Review and Critique; Manuscript: Writing of the first draft, Review and Critique.

REFERENCES

1. Hallett M. Blepharospasm: recent advances. Neurology 2002;59: 1306–1312.
2. Suzuki Y, Mizoguchi S, Kiyosawa M, et al. Glucose hypermetabolism in the thalamus of patients with essential blepharospasm. J Neurol 2007; 254:890–896.
3. Hoire C, Suzuki Y, Kiyosawa M, et al. Decreased dopamine D_2 receptor binding in essential blepharospasm. Acta Neurol Scand 2008; DOI: 0.1111/j.1600–0404. 2008.01053.x.
4. Jankovic J, Orman J. Blepharospasm: demographic and clinical survey of 250 patients. Ann Ophthalmol 1984;16:371–376.
5. Elston JS, Marsden CD, Grandas F, et al. The significance of ophthalmological symptoms in idiopathic blepharospasm. Eye 1988; 2:435–439.
6. McCann JD, Gauthier M, Morschbacher R, et al. A novel mechanism for benign essential blepharospasm. Ophthal Plast Reconstr Surg 1999;15:384–389.
7. Herz NL, Yen MT. Modulation of sensory photophobia in essential blepharospasm with chromatic lenses. Ophthalmology 2005; 112:2208–22011.
8. Anderson RL, Patel BDK, Holds JL, et al. Blepharospasm: past-present-future. Ophthal Plast Reconstr Surg 1998;14:305–317.
9. Adams WH, Digre KB, Patel BC, et al. The evaluation of light sensitivity in benign essential blepharospasm. Am J Ophthalmol 2006;142:82–87.
10. Burstein R, Levy D, Jakubowski M. Effects of sensitization of trigeminovascular neurons to triptan therapy during migraine. Rev Neurol (Paris) 2005;161:658–660.
11. Sherman SM, Guillery RW. Exploring the thalamus. San Diego: Academic Press; 2001.
12. Janavs JL, Aminoff MJ. Dystonia and chorea in acquired systemic disorders. J Neurol Neurosurg Psychiatry 1998;65:436–445.

13. Cusick CG. Anatomical organization of the superior colliculus in monkeys: corticotectal pathways for visual and visuomotor functions. Prog Brain Res 1988;75:1–15.
14. Stein BE, Meredith MA, Wallace MT. The visually responsive neuron and beyond: multisensory integration in cat and monkey. Prog Brain Res 1993;95:79–90.
15. Clarke RJ, Zhang H, Gamlin PD. Characteristics of the pupillary light reflex in the alert rhesus monkey. J Neurophysiol 2003;89: 3179–3189.
16. Esmaeli-Gutstein B, Nahmias C, Thompson M, et al. Positron emission tomography in patients with benign essential blepharospasm. Ophthal Plast Reconstr Surg 1999;15:23–27.
17. Hutchinson M, Nakamura T, Moeller JR, et al. The metabolic topography of essential blepharospasm: a focal dystonia with general implications. Neurology 2000; 55:673–677.
18. Jankovic J, Orman J. Bothlinum A toxin for cranial cervical dystonia: a double-blind, placebo-controlled study. Neurology 1987; 37:616–623.
19. Basso MA, Powers AS, Evinger C. An explanation for reflex blink hyperexcitability in Parkinson's disease. I. Superior colliculus. J Neurosci 1996;16:7308–7317.
20. Vitek JL, Chokkan V, Zhang J-Y, et al. Neuronal activity in the basal ganglia in patients with generalized dystonia and hemiballismus. Ann Neurol 1999;46:22–35.
21. Hikosaka O, Takikawa Y, Kawagoe R. Role of the basal ganglia in the control of purposive saccadic eye movements. Physiol Rev 2000;80:953–978.
22. Quartarone A, Sant'Angelo A, Battaglia F, et al. Enhanced long-term potentiation-like plasticity of the trigeminal blink reflex circuit in blepharospasm. J Neurosci 2006;26:716–721.
23. Ben Simon GJ, Mc Cann JD. Benign essential blepharospasm. Int Ophthalmol Clin 2005;45:49–75.
24. Berardelli A, Rothwell JC, Day BL, et al. Pathophysiology of blepharospasm-oromadibular dystonia. Adv Ophthalmic Plastic Reconstr Surg 1985a;4:87–91.
25. Berardelli A Rothwell JC, Day BL, et al. Pathophysiology of blepharospasm and oromandibular dystonia. Brain 1985b;108:593–608.
26. Demer JL, Holds JB, Hovis LA. Ocular movements in essential blepharospasm. Am J Ophthalmol 1990;110:674–682.
27. Kerrison JB, Lancaster JL, Zamarripa FE, et al. Positron emission tomography scanning in essential blepharospasm. Am J Ophthalmol 2003; 136:846–852.

Acta Neurol Scand DOI: 10.1111/j.1600-0404.2009.01255.x

ACTA NEUROLOGICA
SCANDINAVICA

Cerebrospinal fluid metabolite and nigrostriatal dopaminergic function in Parkinson's disease

Ishibashi K, Kanemaru K, Saito Y, Murayama S, Oda K, Ishiwata K, Mizusawa H, Ishii K. Cerebrospinal fluid metabolite and nigrostriatal dopaminergic function in Parkinson's disease.
Acta Neurol Scand: DOI: 10.1111/j.1600-0404.2009.01255.x.

Objectives – To evaluate the association between cerebrospinal fluid (CSF) homovanillic acid (HVA) concentrations and nigrostriatal dopaminergic function assessed by positron emission tomography (PET) imaging with carbon-11-labeled 2β-carbomethoxy-3β-(4-fluorophenyl)-tropane (^{11}C-CFT), which can measure the dopamine transporter (DAT) density, in Parkinson's disease (PD). *Methods* – ^{11}C-CFT PET scans and CSF examinations were performed on 21 patients with PD, and six patients with non-parkinsonian syndromes (NPS) as a control group. *Results* – In the PD group, CSF HVA concentrations were significantly correlated with the striatal uptake of ^{11}C-CFT ($r = 0.76$, $P < 0.01$). However, in the NPS group, two indices were within the normal range. *Conclusions* – In PD, CSF HVA concentrations correlate with nigrostriatal dopaminergic function. Therefore, CSF HVA concentrations may be an additional surrogate marker for estimating the remaining nigrostriatal dopaminergic function in case that DAT imaging is unavailable.

K. Ishibashi[1,2], K. Kanemaru[3], Y. Saito[4], S. Murayama[5], K. Oda[2], K. Ishiwata[2], H. Mizusawa[1], K. Ishii[2]

[1]Department of Neurology and Neurological Science, Graduate School, Tokyo Medical and Dental University, Tokyo, Japan; [2]Positron Medical Center, Tokyo Metropolitan Institute of Gerontology, Tokyo, Japan; [3]Department of Neurology, Tokyo Metropolitan Geriatric Hospital, Tokyo, Japan; [4]Department of Pathology, Tokyo Metropolitan Geriatric Hospital, Tokyo, Japan; [5]Department of Neuropathology, Tokyo Metropolitan Institute of Gerontology, Tokyo, Japan

Key words: cerebrospinal fluid; dopamine transporter; homovanillic acid; Parkinson's disease; positron emission tomography; ^{11}C-CFT

Kenji Ishii, MD, Positron Medical Center, Tokyo Metropolitan Institute of Gerontology, 1-1 Nakacho, Itabashi-ku, Tokyo 173-0022, Japan
Tel.: +81 3 3964 3241
Fax: +81 3 3964 2188
e-mail: ishii@pet.tmig.or.jp

Accepted for publication June 25, 2009

Introduction

In humans, homovanillic acid (HVA) is the major end-product of dopamine metabolism. The HVA in the cerebrospinal fluid (CSF) is largely derived from the nigrostriatal dopaminergic pathway; therefore, HVA concentration in the CSF has been used as an index of dopamine synthesis and presumed to reflect nigrostriatal dopaminergic function. However, even with the availability of a rigorous collection protocol, especially with respect to puncture time and pre-procedural resting, considerable inter-individual and intra-individual variability has been reported with regard to the concentration of CSF HVA in subjects with normal nigrostriatal function (1–3). Therefore, the extent to which CSF HVA concentrations reflect the nigrostriatal dopaminergic function is still unknown, and no study has specifically elucidated the association between the concentration of CSF HVA and the function of nigrostriatal dopamine.

Many studies have shown that the concentration of CSF HVA substantially reduces in patients with Parkinson's disease (PD), which is a neurodegenerative disorder caused by nigrostriatal dopaminergic dysfunction (4–12). However, the extent of reduction also varied a great deal among patients with PD. Because of the variability, the relationship of clinical disability with CSF HVA concentrations and the accuracy of CSF HVA concentrations in differentiating PD from other parkinsonian syndromes have yet to be determined. Several authors have reported an inverse relationship between CSF HVA concentrations and the clinical severity (5–7, 10, 11), while others have denied such a relationship (9, 12, 13). Other neurodegenerative disorders caused by the dysfunction of nigrostriatal dopaminergic system, such as multiple system atrophy (MSA), progressive

supranuclear palsy (PSP) and corticobasal degeneration, also show the reductions of CSF HVA concentrations as compared to normal subjects (8, 14, 15). Therefore, the usefulness of measuring CSF HVA concentrations in daily clinical practice has not yet been established.

In order to address the physiological and pathophysiological backgrounds of these issues, we evaluated the correlation between CSF HVA concentrations and nigrostriatal dopaminergic function. Furthermore, we have discussed the mechanism by which the concentration of CSF HVA reduces in patients with PD.

As means of evaluating nigrostriatal dopaminergic function, we performed carbon-11-labeled 2β-carbomethoxy-3β-(4-fluorophenyl)-tropane (^{11}C-CFT) positron emission tomography (PET) scans which can reveal the dopamine transporter (DAT) density in the striatum. DAT imaging has been recognized as a standard marker for the diagnosis of PD, because it is a very sensitive, reproducible, and reliable marker of nigrostriatal dopaminergic function (16–21).

Materials and methods

Subjects

The present study was a retrospective study. The subjects comprised 35 patients [19 men and 16 women; age 60–83 years (mean age = 71.7 years, SD = 6.0)]. They visited the neurological outpatient clinic at Tokyo Metropolitan Geriatric Hospital from April 2001–November 2004. Of the 35 patients, 29 had parkinsonian symptoms and on the basis of each clinical criteria (22–24), 21 were diagnosed with PD, three with MSA, and five with PSP. The remaining six patients had no parkinsonian symptoms: three were clinically diagnosed with Alzheimer's disease (AD), two with spinocerebellar degeneration (SCD), and one with amyotrophic lateral sclerosis (ALS). Table 1 shows the demographic data. The patients with MSA and PSP were classified in the patients with non-PD (NPD) group, while the patients with AD, SCD and ALS were classified in the patients with non-parkinsonian syndromes (NPS) group. The CSF examinations and the ^{11}C-CFT PET scans were performed within 5 months of each other. None of the patients had any concomitant hereditary disorder that could cause parkinsonian symptoms. All the patients were drug naive.

The normal range of HVA was determined by examining the CSF of 13 normal control subjects [five men and eight women; age, 65–88 years (mean = 77.2 years, SD = 8.2)]. Similarly, the normal range for nigrostriatal dopaminergic function was determined by performing ^{11}C-CFT PET scans of eight normal control subjects [five men and three women; age, 55–74 years (mean age = 62.3 years, SD = 6.9)]. All the control subjects were healthy and did not have any underlying diseases or abnormities, as determined on the basis of their medical history and their physical and neurological examinations. None of them were on any medications at the time of the study. All the subjects also underwent routine MRI examinations.

All the CSF examinations and ^{11}C-CFT PET scans were performed for research. This study protocol was approved by the Ethics Committee of the Tokyo Metropolitan Institute of Gerontology and written informed consents were obtained from all the participants.

CSF analysis

Lumbar puncture was performed in the lateral decubitus position to obtain CSF samples from each subject. The first few milliliter of CFS was discarded. The next 3 ml of CFS was used for routine determinations of cell counts, protein and sugar and an additional 2 ml was stored at −70°C until the assays were preformed. The concentration of CSF HVA was measured by injecting 80 μl CSF

Table 1 Demographics of patients and control subjects

	Subjects					
	n	M:F	Age (years)	Duration (years)	Striatal uptake of ^{11}C-CFT (Uptake ratio index)	CSF HVA (ng/ml)
Parkinson's disease	21	11:10	72.9 ± 5.0	1.8 ± 1.3	0.94 ± 0.20	12.8 ± 9.35
Hoehn-Yahr 1	1	1:0	62	1	1.38	36.8
Hoehn-Yahr 2	8	4:4	71.6 ± 4.6	1.4 ± 0.9	1.03 ± 0.14	15.6 ± 9.4
Hoehn-Yahr 3	12	6:6	74.7 ± 3.9	2.1 ± 1.5	0.85 ± 0.17	8.9 ± 5.4
Non-Parkinson's disease	8	4:4	70.5 ± 7.7	1.6 ± 0.8	1.00 ± 0.19	16.4 ± 7.7
Non-parkinsonian syndromes	6	4:2	68.8 ± 6.3	4.5 ± 2.4	2.48 ± 0.28	31.9 ± 13.0
Control for PET study	8	5:3	62.3 ± 6.9		2.68 ± 0.44	
Control for CSF study	13	5:8	77.2 ± 8.2			36.0 ± 13.8

Data are expressed as mean ± SD; *n* = number, CSF, cerebrospinal fluid; HVA, homovanillic acid.

samples into a high-performance liquid chromatography system equipped with 16 electrochemical sensors (CEAS Model 5500; ESA, Bedford, MA, USA), as described previously (14).

PET imaging

^{11}C-CFT PET data acquisition – PET studies were performed at the Positron Medical Center, Tokyo Metropolitan Institute of Gerontology using a SET 2400W scanner (Shimadzu, Kyoto, Japan) in the three-dimensional scanning mode (25). The ^{11}C-CFT was prepared as described previously (26). Each subject received an intravenous bolus injection of 388 ± 75 (mean ± SD) MBq of ^{11}C-CFT. Each subject was then placed in the supine position with their eyes closed in the PET camera gantry. The head was immobilized with a customized head holder in order to align the orbitomeatal line parallel to the scanning plane. To measure the uptake of ^{11}C-CFT, a static scan was performed for 75–90 min after the injection. The specific activity at the time of injection ranged from 7.1–119.6 GBq/μmol. The transmission data were acquired using a rotating ^{68}Ga/^{68}Ge rod source for attenuation correction. Images of 50 slices were obtained with a resolution of 2 × 2 × 3.125 mm voxels and a 128 × 128 matrix.

Analysis of ^{11}C-CFT PET images – Image manipulations were carried out by using the Dr View software (version R2.0; AJS, Tokyo, Japan). The individual PET images were resliced in the transaxial direction, parallel to the anterior–posterior intercommissural (AC–PC) line. Circular regions of interest (ROIs) were placed with reference to the brain atlas and individual MRI images. Five ROIs (diameter, 8 mm) were placed on the striatum on both the left and right sides in each of the three contiguous slices (the AC–PC plane, and regions 3.1 and 6.2 mm above the AC–PC line). Of the five ROIs, one ROI was placed on the caudate and four on the putamen. A total of 50 ROIs (diameter, 10 mm) were selected throughout the cerebellar cortex in five contiguous slices. To evaluate the striatal uptake of ^{11}C-CFT, we calculated the uptake ratio index by the following formula (17, 18), as previously validated (27, 28).

$$\text{Uptake ratio index} = (\text{activity in the striatum} - \text{activity in the cerebellum}) / (\text{activity in the cerebellum}).$$

Statistical analysis

Differences in the averages were tested using a Student's *t*-test. Correlations between the two groups were assessed by linear regression analysis with Pearson's correlation test. $P < 0.01$ was considered to indicate statistical significance.

Results

The inter-individual variability in the concentrations of CSF HVA in each group was relatively large (Fig. 1A). CSF HVA concentrations in both the PD ($P < 0.01$) and NPD groups ($P < 0.01$) were significantly lower than that in the control group (mean ± 2SD, 36.0 ± 27.6), while no significant difference was observed between the NPS and control groups.

The striatal uptake of ^{11}C-CFT in the PD and NPD groups was below the normal range (mean ± 2SD, 2.68 ± 0.87; Fig. 1B). In the PD group, CSF HVA concentrations were significantly

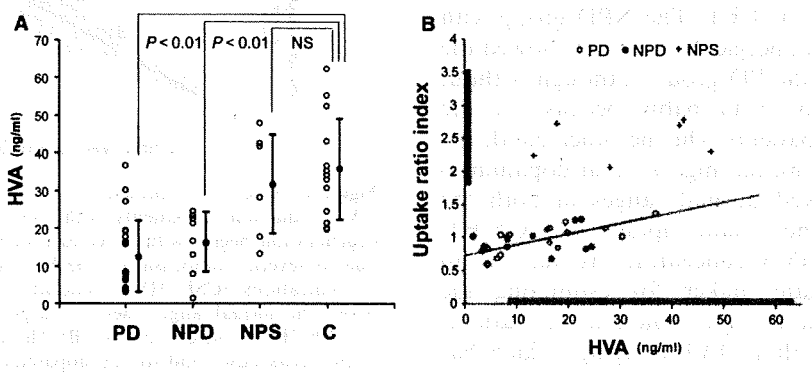

Figure 1. (A) The comparison of CSF HVA concentrations among the disease and control groups. Vertical bars represent mean ± SD. (B) Relationship between CSF HVA concentrations and the striatal uptake of ^{11}C-CFT. A solid line represents the regression line for the PD group. Linear correlation was significant ($r = 0.76$; $P < 0.01$). The grey bars beside the *x*- and *y*-axes represent the normal range (mean ± 2SD) for HVA (36.0 ± 27.6) and the striatal uptake of ^{11}C-CFT (2.68 ± 0.87). PD, Parkinson's disease; NPD, non-Parkinson's disease with parkinsonism; NPS, non-parkinsonian syndromes; C, controls; NS, not significant; CSF, cerebrospinal fluid; HVA, homovanillic acid.

correlated with the striatal uptake of ^{11}C-CFT ($r = 0.76$, $P < 0.01$). In the NPD group, although the correlation between the two indices was not statistically significant, the distribution pattern between the two indexes showed the same tendency as that in the PD group. However, in the NPS group, both CSF HVA concentrations and the striatal uptake of ^{11}C-CFT were within the normal ranges.

Discussion

We evaluated the correlation between CSF HVA concentrations and nigrostriatal dopaminergic function by performing ^{11}C-CFT PET scans. ^{11}C-CFT PET scans showed that all patients with PD and NPD had the dysfunction of nigrostriatal dopaminergic system and all patients with NPS had normal function. The CSF HVA concentrations of all patients with PD and NPD were significantly lower than those of normal subjects, in accordance with previous studies (5–12, 14, 15), whereas, there was no significant difference in CSF HVA concentrations between normal subjects and patients with NPS. These results suggest that CSF HVA concentrations could reflect nigrostriatal dopaminergic function. However, in accordance with previous reports (1–9, 13, 14), all groups showed large inter-individual variability in CSF HVA concentrations and relatively wide overlaps among groups were found. Therefore, in clinical practice, measuring CSF HVA concentrations may be of limited value in the diagnosis of PD.

This is the first study that investigated the correlation between CSF HVA concentrations and nigrostriatal dopaminergic dysfunction. Regardless of relatively high inter-individual variability, CSF HVA concentrations in the PD group showed a considerably high correlation with the striatal uptake of ^{11}C-CFT. The NPD group with nigrostriatal dopaminergic dysfunction showed the same tendency as the PD group, although without significant correlation probably because of the small number of patients. On the other hand, the NPD group with normal nigrostriatal dopaminergic function showed normal ranges in both the HVA level and the striatal uptake of ^{11}C-CFT. Therefore, CSF HVA concentrations may be an additional surrogate maker for estimating the nigrostriatal dopaminergic function in patients with PD, in case that DAT imaging, which has been recognized as a standard maker for the diagnosis of PD, is unavailable.

It is important to note that the DAT images of patients with PD are unique; in the pre-symptomatic phase the reduction in the availability of striatal DAT was detected, presumably as a result of both the degeneration of nigral dopaminergic cells and the compensatory downregulation of DATs on the presynaptic site to maintain normal synaptic dopamine concentrations (17–21). Furthermore, the striatal DAT availability declined at an annual rate of 5–10% (19, 21, 29–31).

Considering our results and the unique characteristics of the DAT images, a possible explanation about the association between CSF HVA concentrations and the striatal uptake of ^{11}C-CFT is as follows (Fig. 2). The first stage of the disease is a compensatory and asymptomatic phase. Along with the progression of nigrostriatal degeneration, the striatal DAT availability begins to decrease, as described earlier (17–21). However, due to several compensatory mechanisms, including the downregulation of DATs and the upregulation of dopamine synthesis, the striatal dopamine concentrations are kept within the normal range (32). As a result, CSF HVA concentrations are also kept in the normal range because CSF HVA is the major end-product of striatal dopamine metabolism. This phase would show relatively large intra-individual and inter-individual variability in CSF HVA concentrations, as observed in subjects with normal nigrostriatal dopaminergic function, because of the reserve capacity for adjusting its levels. The second stage of the progression of the disease is an advanced and symptomatic phase. The compensatory mechanisms to maintain normal synaptic

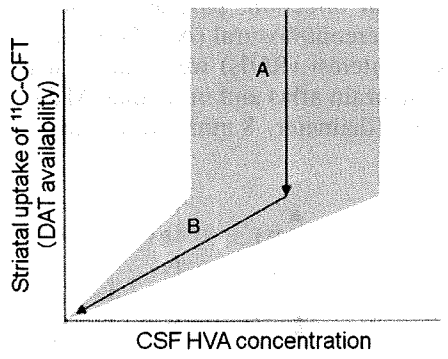

Figure 2. Schematic representation of the mechanism of CSF HVA reduction in patients with PD. (A) The nigrostriatal degeneration begins with a decrease in DAT availability, but due to several compensatory mechanisms, striatal dopamine concentrations (CSF HVA concentrations) are maintained within the normal range. There is a large variability with regard to CSF HVA concentrations. (B) The compensatory mechanisms break down and striatal dopamine concentrations (CSF HVA concentrations) begin to decrease along with the decrease in DAT availability. The variability in CSF HVA concentrations gradually becomes smaller. The grey zone represents the range of variability in CSF HVA concentrations to the striatal uptake of ^{11}C-CFT. DAT, dopamine transporter; CSF, cerebrospinal fluid, HVA, homovanillic acid.

dopamine concentrations break down and the striatal dopamine and CSF HVA concentrations begin to decrease with the reduction of DAT availability. In this phase, the intra-individual and inter-individual variability in CSF HVA concentrations would gradually decrease because of a lesser capacity for adjusting its levels. Consequently, CSF HVA concentrations remain within a narrow range that corresponds to the remaining nigrostriatal dopaminergic function. In symptomatic patients with PD, CSF HVA concentrations correlate with nigrostriatal dopaminergic function. To verify this explanation, a study with larger number of patients is needed.

In conclusion, we found a significant correlation between CSF HVA concentrations and the striatal uptake of ^{11}C-CFT in patients with PD. Although we should remember that CSF HVA concentrations show large variability, CSF HVA concentrations may be an additional surrogate maker for estimating the remaining nigrostriatal dopaminergic function in patients with PD in case that DAT imaging is unavailable.

Acknowledgements

The authors thank Mr Keiichi Kawasaki and Ms Hiroko Tsukinari for their technical assistance. This study was supported by Grants-in-Aid for Neurological and Psychiatric Research (S. Murayama, Y. Saito and K. Ishii) and Research for Longevity (S. Murayama, Y. Saito and K. Ishii) from the Ministry of Health, Labor and Welfare of Japan; for Scientific Research (B) No. 20390334 (K. Ishiwata) from the Japan Society for the Promotion of Science; for the Program for Promotion of Fundamental Studies in Health Sciences of the National Institute of Biomedical Innovation, Japan (No: 06–46, K. Ishiwata); and for Long-Term Comprehensive Research on Age-associated Dementia from the Tokyo Metropolitan Institute of Gerontology (K. Kanemaru, S. Murayama and K. Ishii).

References

1. Seeldrayers P, Messina D, Desmedt D, Dalesio O, Hildebrand J. CSF levels of neurotransmitters in Alzheimer-type dementia. Effects of ergoloid mesylate. Acta Neurol Scand 1985;**71**:411–4.
2. Ballenger JC, Post RM, Goodwin FK. Neurochemistry of cerebrospinal fluid in normal individuals. In: Wood JH, ed. Neurobiology of cerebrospinal fluid. New York: Plenum Press, 1982;**2**:143–55.
3. Hildebrand J, Bourgeois F, Buyse M, Przedborski S, Goldman S. Reproducibility of monoamine metabolite measurements in human cerebrospinal fluid. Acta Neurol Scand 1990;**81**:427–30.
4. Parkinson Study Group. Cerebrospinal fluid homovanillic acid in the DATATOP study on Parkinson's disease. Parkinson Study Group. Arch Neurol 1995;**52**:237–45.
5. Chia LG, Cheng FC, Kuo JS. Monoamines and their metabolites in plasma and lumbar cerebrospinal fluid of Chinese patients with Parkinson's disease. J Neurol Sci 1993;**116**:125–34.
6. Chase TN, Ng LK. Central monoamine metabolism in Parkinson's disease. Arch Neurol 1972;**27**:486–91.
7. Korf J, van Praag HM, Schut D, Nienhuis RJ, Lakke JP. Parkinson's disease and amine metabolites in cerebrospinal fluid: implications for L-Dopa therapy. Eur Neurol 1974; **12**:340–50.
8. Abdo WF, De Jong D, Hendriks JC et al. Cerebrospinal fluid analysis differentiates multiple system atrophy from Parkinson's disease. Mov Disord 2003;**19**:571–9.
9. Davidson DL, Yates CM, Mawdsley C, Pullar IA, Wilson H. CSF studies on the relationship between dopamine and 5-hydroxytryptamine in Parkinsonism and other movement disorders. J Neurol Neurosurg Psychiatry 1977;**40**: 1136–41.
10. Tohgi H, Abe T, Takahashi S, Ueno M, Nozaki Y. Cerebrospinal fluid dopamine, norepinephrine, and epinephrine concentrations in Parkinson's disease correlated with clinical symptoms. Adv Neurol 1990;**53**:277–82.
11. Mayeux R, Stern Y. Intellectual dysfunction and dementia in Parkinson disease. Adv Neurol 1983;**38**:211–27.
12. Gibson CJ, Logue M, Growdon JH. CSF monoamine metabolite levels in Alzheimer's and Parkinson's disease. Arch Neurol 1985;**42**:489–92.
13. Kurlan R, Goldblatt D, Zaczek R et al. Cerebrospinal fluid homovanillic acid and parkinsonism in Huntington's disease. Ann Neurol 1988;**24**:282–4.
14. Kanemaru K, Mitani K, Yamanouchi H. Cerebrospinal fluid homovanillic acid levels are not reduced in early corticobasal degeneration. Neurosci Lett 1998;**245**:121–2.
15. Ruberg M, Javoy-Agid F, Hirsch E et al. Dopaminergic and cholinergic lesions in progressive supranuclear palsy. Ann Neurol 1985;**18**:523–9.
16. Nurmi E, Bergman J, Eskola O et al. Reproducibility and effect of levodopa on dopamine transporter function measurements: a [18F]CFT PET study. J Cereb Blood Flow Metab 2000;**20**:1604–9.
17. Frost JJ, Rosier AJ, Reich SG et al. Positron emission tomographic imaging of the dopamine transporter with 11C-WIN 35,428 reveals marked declines in mild Parkinson's disease. Ann Neurol 1993;**34**:423–31.
18. Wong DF, Yung B, Dannals RF et al. In vivo imaging of baboon and human dopamine transporters by positron emission tomography using [11C]WIN 35,428. Synapse 1993;**15**:130–42.
19. Nurmi E, Bergman J, Eskola O et al. Progression of dopaminergic hypofunction in striatal subregions in Parkinson's disease using [18F]CFT PET. Synapse 2003; **48**:109–15.
20. Rinne JO, Ruottinen H, Bergman J, Haaparanta M, Sonninen P, Solin O. Usefulness of a dopamine transporter PET ligand [(18)F]beta-CFT in assessing disability in Parkinson's disease. J Neurol Neurosurg Psychiatry 1999;**67**:737–41.
21. Nurmi E, Ruottinen HM, Kaasinen V et al. Progression in Parkinson's disease: a positron emission tomography study with a dopamine transporter ligand [18F]CFT. Ann Neurol 2000;**47**:804–8.
22. Hughes AJ, Daniel SE, Kilford L, Lees AJ. Accuracy of clinical diagnosis of idiopathic Parkinson's disease: a clinico-pathological study of 100 cases. J Neurol Neurosurg Psychiatry 1992;**55**:181–4.
23. Litvan I, Agid Y, Calne D et al. Clinical research criteria for the diagnosis of progressive supranuclear palsy (Steele-Richardson-Olszewski syndrome): report of the NINDS-SPSP international workshop. Neurology 1996; **47**:1–9.

24. Gilman S, Low PA, Quinn N et al. Consensus statement on the diagnosis of multiple system atrophy. J Auton Nerv Syst 1998;**74**:189–92.
25. Fujiwara T, Watanuki S, Yamamoto S et al. Performance evaluation of a large axial field-of-view PET scanner: SET-2400W. Ann Nucl Med 1997;**11**:307–13.
26. Kawamura K, Oda K, Ishiwata K. Age-related changes of the [11C]CFT binding to the striatal dopamine transporters in the Fischer 344 rats: a PET study. Ann Nucl Med 2003;**17**:249–53.
27. Hashimoto M, Kawasaki K, Suzuki M et al. Presynaptic and postsynaptic nigrostriatal dopaminergic functions in multiple system atrophy. Neuroreport 2008;**19**:145–50.
28. Ishibashi K, Ishii K, Oda K, Kawasaki K, Mizusawa H, Ishiwata K. Regional analysis of age-related decline in dopamine transporters and dopamine D(2)-like receptors in human striatum. Synapse 2008;**63**:282–90.
29. Staffen W, Mair A, Unterrainer J, Trinka E, Ladurner G. Measuring the progression of idiopathic Parkinson's disease with [123I] beta-CIT SPECT. J Neural Transm 2000; **107**:543–52.
30. Chouker M, Tatsch K, Linke R, Pogarell O, Hahn K, Schwarz J. Striatal dopamine transporter binding in early to moderately advanced Parkinson's disease: monitoring of disease progression over 2 years. Nucl Med Commun 2001;**22**:721–5.
31. Marek K, Innis R, van Dyck C et al. [123I]beta-CIT SPECT imaging assessment of the rate of Parkinson's disease progression. Neurology 2001;**57**:2089–94.
32. Lee CS, Samii A, Sossi V et al. In vivo positron emission tomographic evidence for compensatory changes in presynaptic dopaminergic nerve terminals in Parkinson's disease. Ann Neurol 2000;**47**:493–503.

International Journal of Neuropsychopharmacology (2009), **12**, 1127–1131. Copyright © CINP 2009
doi:10.1017/S1461145709990204

BRIEF REPORT

CINP

High occupancy of σ_1 receptors in the human brain after single oral administration of donepezil: a positron emission tomography study using [^{11}C]SA4503

Masatomo Ishikawa[1,2,3], Muneyuki Sakata[2], Kenji Ishii[2], Yuichi Kimura[4], Keiichi Oda[2], Jun Toyohara[1,2], Jin Wu[1,2], Kiichi Ishiwata[2], Masaomi Iyo[3] and Kenji Hashimoto[1]

[1] *Division of Clinical Neuroscience, Chiba University Center for Forensic Mental Health, Chiba, Japan*
[2] *Positron Medical Center, Tokyo Metropolitan Institute of Gerontology, Tokyo, Japan*
[3] *Department of Psychiatry, Chiba University Graduate School of Medicine, Chiba, Japan*
[4] *Molecular Imaging Center, National Institute of Radiological Sciences, Chiba, Japan*

Abstract

The acetylcholinesterase (AChE) inhibitor donepezil is also a σ_1 receptor agonist. We examined whether donepezil binds to σ_1 receptors in the living human brain after a single oral administration. Dynamic positron emission tomography (PET) data acquisition using the selective σ_1 receptor ligand [^{11}C]SA4503 was performed to evaluate quantitatively the binding of [^{11}C]SA4503 to σ_1 receptors in eight healthy male volunteers. Each subject had a PET scan before and after receiving a single dose of donepezil (5 or 10 mg). The binding potential of [^{11}C]SA4503 was calculated. Doses of 5 mg and 10 mg donepezil bound to σ_1 receptors in the human brain with occupancies of ~60% and ~75%, respectively, in a dose-dependent manner. This study demonstrated that donepezil binds to σ_1 receptors in the living human brain at therapeutic doses. Therefore, σ_1 receptors may be implicated in the pharmacological mechanism of donepezil in the human brain.

Received 28 April 2009; Reviewed 12 May 2009; Revised 27 May 2009; Accepted 29 May 2009; First published online 2 July 2009

Key words: Acetylcholinesterase inhibitor, donepezil, PET, σ_1 receptor, [^{11}C]SA4503.

Introduction

Donepezil, an acetylcholinesterase (AChE) inhibitor, is the most widely prescribed drug for Alzheimer's disease (Blennow *et al.* 2006). In addition to AChE inhibition, donepezil also binds to sigma (σ) receptors with high affinity (IC_{50} = 14.6 nM), although the radioligand [^{3}H]DTG (for σ_1 and σ_2 receptors) used in this study is not selective for σ_1 receptors (Kato *et al.* 1999). Accumulating evidence suggest that σ_1 receptors play a role in the pathophysiology of neuropsychiatric diseases, including Alzheimer's disease, schizophrenia, and major depression (Hashimoto & Ishiwata, 2006; Hayashi & Su, 2004). Interestingly, it has been demonstrated that σ_1 receptors are implicated in the anti-amnesic and neuroprotective effects of donepezil against learning impairments induced by the *N*-methyl-D-aspartate receptor antagonist dizocilpine (Maurice *et al.* 2006) and against amyloid β_{25-35} peptide-induced neurotoxicity (Meunier *et al.* 2006) in mice. Recently, we reported that donepezil, but not physostigmine, significantly potentiated the nerve growth factor-induced neurite outgrowth in PC12 cells, and that potentiation of nerve growth factor-induced neurite outgrowth by donepezil was significantly blocked by co-administration of the selective σ_1 receptor antagonist NE-100 (Ishima *et al.* 2008). Taken together, these results suggest that the pharmacological actions of donepezil as both an AChE inhibitor and σ_1 receptor agonist probably contribute to the efficacy of this drug in patients with Alzheimer's disease (Ishima *et al.* 2008; Maurice *et al.* 2006; Meunier *et al.* 2006).

Address for correspondence: Dr K. Hashimoto, Division of Clinical Neuroscience, Chiba University Center for Forensic Mental Health, 1-8-1 Inohana, Chiba 260-8670, Japan.
Tel.: +81-43-226-2147 *Fax*: +81-43-226-2150
Email: hashimoto@faculty.chiba-u.jp

Positron emission tomography (PET) is the most effective technique to estimate the receptor occupancy by drugs in the human brain. SA4503 has an affinity of ~17.4 nM (IC_{50}) for the σ_1 receptor, which is about 100 times higher than those for σ_2, α_1-adrenergic, dopamine D_2, serotonin $(5\text{-HT})_{1A}$, 5-HT_2, histamine H_1, muscarinic M_1, and musicarinic M_2 receptors, and has no affinity for other 29 receptors, ion channels, and second-messenger systems (Matsuno *et al.* 1996). Using PET and [^{11}C]SA4503 (Kawamura *et al.* 2000), Ishiwata *et al.* (2006) reported a high occupancy by the typical antipsychotic drug haloperidol (3 mg) for σ_1 receptors (~80%) as well as dopamine D_2 receptors (~60%) in the human brain after a single oral administration. Furthermore, we reported a high occupancy of σ_1 receptors (~60%) in the human brain after a single oral administration of fluvoxamine, a selective serotonin reuptake inhibitor, using [^{11}C]SA4503 PET, suggesting that σ_1 receptors may be implicated in the mechanisms of action of fluvoxamine (Ishikawa *et al.* 2007). These studies demonstrate that [^{11}C]SA4503 PET is useful for evaluation of σ_1 receptor occupancy by therapeutic drugs in the human brain (Ishikawa *et al.* 2007; Ishiwata *et al.* 2006).

The purpose of this study was to determine whether donepezil binds to σ_1 receptors in the human brain by using [^{11}C]SA4503 PET.

Methods

This study was approved by the Ethical Committee of the Tokyo Metropolitan Institute of Gerontology and the Ethics Committee of the Chiba University Graduate School of Medicine. Eight healthy Japanese male volunteers participated in the study (mean age = 33.0 yr, S.D. = 8.6 yr, range = 24–46 yr) after providing written informed consent. None of the subjects had any neurological or psychological findings, or showed any abnormalities in the brain magnetic resonance imaging scan taken between the two PET scans. None had been receiving any medications of any kind. None had a history of alcoholism. Each volunteer participated in two [^{11}C]SA4503 PET scans, one before and one after a single oral administration of donepezil (Aricept® 5 mg or 10 mg tablet; Eisai Co. Ltd, Japan). Twenty-six arterial blood samples were collected during each PET scan and were used as the input function. Either a 5 mg or a 10 mg donepezil tablet was administered randomly within 5 min of the end of the first (baseline) PET scan. The second (donepezil-loading) PET scan took place 3–3.5 h after taking donepezil to coincide with the peak plasma level (T_{max} = ~3.5 h) in healthy male Japanese subjects (Ohnishi *et al.* 1993). Blood samples were collected just before the tracer injection of the second PET scan to determine the plasma concentration of donepezil. The plasma concentration of donepezil was measured by high-performance liquid chromatography.

[^{11}C]SA4503 was prepared as described previously (Kawamura *et al.* 2000). Ninety-minute PET scans were carried out using previously described methods (Ishikawa *et al.* 2007; Ishiwata *et al.* 2006). Regions of interest (ROIs) were defined over the frontal, temporal, parietal, occipital and anterior cingulate cortices, head of the caudate nucleus, putamen, thalamus, hippocampus, and cerebellum with reference to the co-registered magnetic resonance images.

Binding of [^{11}C]SA4503 to σ_1 receptors was calculated as the binding potential (BP_{ND}) (Innis *et al.* 2007) with methods described elsewhere (Sakata *et al.* 2007) with slight modifications. Briefly, the BP_{ND} was determined using a two-tissue three-compartment model (Mintun *et al.* 1984). The modifications were employment of two constraints for more stable estimations: the rate K_1/k_2 in the model is constant in each scan and this rate is not affected by donepezil. The σ_1 receptor occupancy (%) by donepezil was calculated for each ROI as

$$100 \times \frac{BP_{ND} \text{ at baseline} - BP_{ND} \text{ at donepezil loading}}{BP_{ND} \text{ at baseline}}.$$

Images of the total volume of distribution (V_T) of [^{11}C]SA4503 were calculated using the Logan plot method (Logan *et al.* 1996; Sakata *et al.* 2007). V_T is a good reflection of the BP_{ND} in the case of [^{11}C]SA4503 (Kimura *et al.* 2007).

The equation

$$Occ = Occ_{max}(F/(F + ED_{50})),$$

where Occ refers to occupancy, F refers to blood level of donepezil, Occ_{max} is the maximal receptor occupancy and ED_{50} is the blood donepezil level resulting in 50% maximal receptor occupancy, was used to evaluate the relationship between σ_1 receptor occupancy and the blood concentration of donepezil.

The data are presented as means ± S.D. Statistical analysis was performed with SPSS software package version 12.0 J (SPSS Inc., Japan). Concentration-dependent relationships were evaluated by nonlinear regression analysis.

Results

Representative parametric images of V_T of [^{11}C]SA4503 before and after donepezil (10 mg) loading are shown in Fig. 1. A single administration of